J Mater Sci (2008) 43:5982–5988
DOI 10.1007/s10853-008-2748-1

Catalytic behavior of niobia species on oxidation reactions: insights from experimental and theoretical models

Teodorico C. Ramalho · Luiz C. A. Oliveira · Kele T. G. Carvalho · Eugênio F. Souza · Elaine F. F. da Cunha · Marcelo Nazzaro

Received: 25 November 2007 / Accepted: 21 May 2008 / Published online: 13 August 2008

Abstract This paper describes the preparation and use of a new class of material based on synthetic Niobia as catalysts in oxidizing reactions of organic compounds in aqueous medium. The reaction chemicals were carried out in presence of hydrogen peroxide (H_2O_2). The material was characterized with X-ray diffraction, XPS, and UV–Vis measurements. The organic molecule methylene-blue was used in decomposition study as probe contaminant. The analysis using the ESI-MS technique showed complete oxidation observed through different intermediates. This suggests the use of Niobia species as efficient Fenton-like catalyst in degradation reactions. Theoretical quantum DFT calculations were carried out in order to understand the degradation mechanism.

Introduction

It has been reported that niobium is interesting and important for some catalytic reactions, and then the research and development of niobium compounds in catalytic applications have increased in recent years [1]. However, the use of pure niobium oxides as a catalyst for the oxidation of contaminants in aqueous medium is scarce in bibliography. It has been reported a study with niobium oxides as a catalyst for hydroxylation, but combined with an inorganic cation at high temperature [2]. In general, research focuses on the study of the catalytic performance of Nb_2O_5 impregnated with metal oxides [3]. The particular properties of the niobium, such as, redox properties, photosensitivity, acidity, and catalytic behavior [4], constitute the motivation to understand and use niobium for catalytic purposes. Some important materials were been used as catalyst supports or promoters, but we are interesting in the utilization of Niobia. The natural abundance of niobium in the Earth crust is about 20 ppm in mass. Distributed by country, Brazil is the main niobium supplier, providing about 60% of the world production. Despite of the increasing interest on applications of niobium compounds in many technological fields, the niobium chemistry is not as deeply dominated for other more common industrial metals, as in heterogeneous catalysis [5]. Niobium-based materials are effective catalysts in numerous reactions, such as pollution control, selective oxidation, hydrogenation and dehydrogenation, dehydration and hydration, photochemistry, electrochemistry, and polymerization. A remarkable application of niobium-based compounds is on oxidation catalysis such as Fenton reaction. Fenton reaction involving hydrogen peroxide and ferrous catalyst is currently one of the most powerful oxidizing reactions available [6].

The main purpose of this paper was to prepare a new class of material based on a natural niobium oxide (niobia) to act as catalyst on the textile dye oxidation through a Fenton-like mechanism. In addition, some experiments have been carried out in order to study the effects of natural and synthetic Nb_2O_5 on the degradation of organic dye in the presence of hydrogen peroxide. The reaction mechanism of the heterogeneous dye/niobia/H_2O_2 system has been studied on-line by ESI-MS and theoretical calculations.

T. C. Ramalho (✉) · L. C. A. Oliveira · K. T. G. Carvalho · E. F. Souza · E. F. F. da Cunha
Departamento de Química, Universidade Federal de Lavras, Caixa Postal, CEP 37200-000 Lavras, MG, Brazil
e-mail: teo@ufla.br

L. C. A. Oliveira
e-mail: luizoliveira@ufla.br

M. Nazzaro
Laboratorio de Ciencias de Superficies y Medios Porosos, Departamento de Física, UNSL, 5700 San Luis, Argentina

Methodology

Materials and characterization

In this study two different materials were utilized for the oxidation reaction in the presence of H_2O_2: (i) a synthetic niobia prepared in our laboratory (synthetic niobia) and (iii) this synthetic niobia previously treated with H_2O_2 (30% v/v), called synthetic niobia//H_2O_2. Synthetic niobia was prepared from $NH_4[NbO(C_2O_4)_2(H_2O)](H_2O)_n$ (supplied by CBMM—Companhia Brasileira de Metalurgia e Mineração, Araxá-MG) and NaOH (50 mL, 1 mol L^{-1}) by co-precipitation followed by thermal treatment at 60 °C (72 h) [7]. The synthetic niobium oxide (synthetic niobia) was previously treated with H_2O_2 to produce the sample niobia//H_2O_2. This sample was prepared by treatment of synthetic niobia (3 g) with hydrogen peroxide 30% v/v (10 mL) at 25 °C for 1 h.

The powder X-ray diffraction (XRD) data were obtained in a Rigaku model Geigerflex using Cu Kα radiation scanning from 2 to 75° at a scan rate of 4° min^{-1}. XPS data were obtained by KRATOS Analytical XSAM 800 cpi ESCA equipped with a Mg anode (Mg Kα radiation, 1,253.6 eV) and spherical analyzer operating at 15 kV and 15 mA.

Experimental degradation tests were carried out at 25 °C using methylene blue dye (50 mg L^{-1}) and niobia catalyst (10 mg L^{-1}) in an oxidant solution comprised of H_2O_2 (97 mmol). The oxidant solution was stirred for 2 min before mixing with the dye and the niobia. The reactions were monitored by UV–Vis measurements (Shimadzu-UV-1601 PC). All the reactions were carried out under magnetic stirring in a recirculating temperature-controlled bath kept at 25 ± 1 °C.

Studies by ESI-MS

In an attempt to identify the intermediate formation, the methylene blue decomposition was also monitored with the positive ion mode ESI-MS of an Agilent MS-ion trap mass spectrometer. The reaction samples were analyzed by introducing aliquots into the ESI source with a syringe pump at a flow rate of 5 mL min^{-1}. The spectra were obtained as an average of 50 scans of 0.2 s. Typical ESI conditions were as follows: heated capillary temperature 1,508 °C; sheath gas (N_2) at a flow rate of 20 units (ca. 4 L min^{-1}); spray voltage 4 kV; capillary voltage 25 V; tube lens offset voltage 25 V.

Computational methods

The calculations were carried out with the package *Gaussian98* [8]. All the transition states, intermediates, and precursors involved were calculated. Each conformer was fully optimized by DFT. The energy profile at selected DFT geometries along the reaction pathway has been computed at B3LYP level of theory using the 6-31+G (d,p) basis set. This computational procedure has been employed previously on similar systems with success [9, 10]. Furthermore, after each optimization the nature of each stationary point was established by calculating and diagonalizing the Hessian matrix (force constant matrix). The unique imaginary frequency associated with the transition vector [7], i.e., the eigenvector associated with the unique negative eigenvalue of the force constant matrix, has been characterized. The solvent effect was evaluated with utilization of polarized continuum model salvation calculations, initially proposed by Barone et al. [11] and Tomasi et al. [12]. The final structures were submitted to analysis of natural bound order (NBO) [13, 14] with the density functional Becke's three-parameter exchange functional and the gradient-corrected functional of Lee, Yang, and Paar (B3LYP) using the basis set 6-311G** [15]. All the minima connected by a given transition state were confirmed by intrinsic reaction coordinate-driving calculations [16] (in mass-weighted coordinates) as implemented in GAUSSIAN03 program [17].

For all the studied species, we have checked $S2$ values to evaluate whether spin contamination can influence the quality of the results. In all the cases we have found that the calculated values differ from $S(S + 1)$ by less than 10%.

Results and discussion

Characterization

XRD patterns for the samples indicate that the materials are amorphous. These results are in very good agreement with other experimental studies [18].

The samples were characterized using XPS techniques, the spectra are reported in Fig. 1a. The XPS Nb3d5/2 spectra of the pure niobia and niobia treated with hydrogen peroxide (Fig. 1) are very similar and show the same peaks from Nb_2O_5 reported in literature. It means that the treatment with H_2O_2 does not change the structure of the niobium species significantly. The two well-defined peaks at 207.1 and 209.8 eV correspond to the reported binding energies of Nb_2O_5. The reduction of the niobium does not showed in XPS analysis (Nb 3d) probably due to formation of unstable phases ($Nb^{5-\delta}$) with the partial reduction, but a significantly difference can be observed in the XPS profile from O 1s spectrum. The spectrum from the synthetic niobia showed only one peak at 529.9 eV related to the oxygen anions (O_2^-) bound to the niobium in the lattice. From the synthetic niobia//H_2O_2, the main peak at

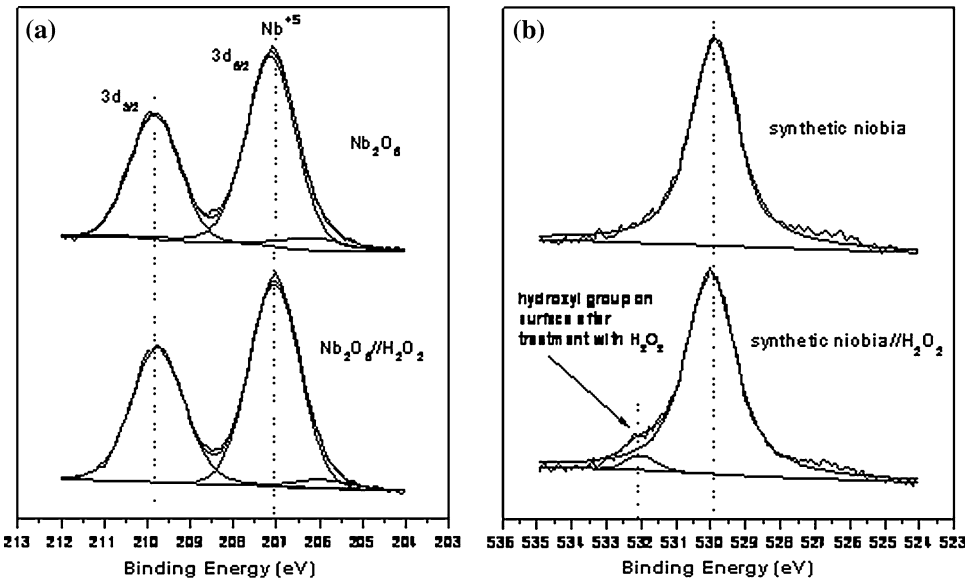

Fig. 1 XPS profiles of Nb 3d (**a**) and O 1s region of synthetic niobia (**b**)

529.9 eV is accompanied by a peak at 532.1 eV attributed to the formation of hydroxyl groups on the niobia surface (Fig. 1b). The formation of hydroxyl groups on the niobia surface was also identified by the XPS O 1s spectrum and reported by Oliveira et al. [18].

Catalytic studies

It was then studied the oxidation of the textile dye methylene blue with H_2O_2 in presence of the synthetic niobia and synthetic niobia//H_2O_2. It has been observed with the synthetic niobia catalyst a slight discoloration is observed at the beginning, followed by a significant discoloration (Fig. 2) after 90 min of reaction. Total discoloration took place after 150 min. This sample, after a previous treatment with hydrogen peroxide (niobia//H_2O_2), showed a strong discoloration at 90 min, indicating that the treatment

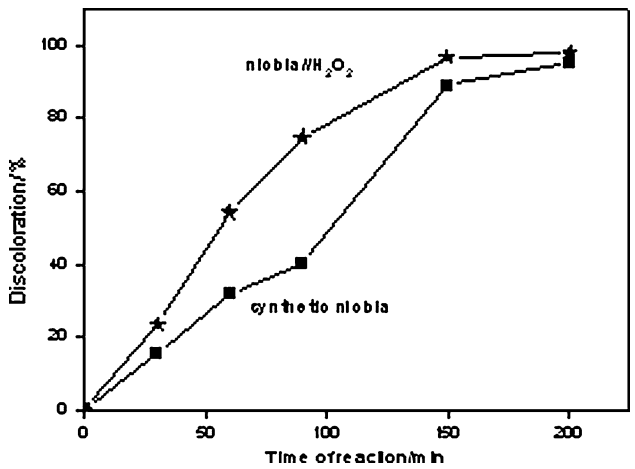

Fig. 2 Discoloration of methylene blue dye with niobia and hydrogen peroxide monitored by UV-Visible spectrometry

with H_2O_2 improves the catalytic activity in the oxidation of the dye.

The identification of reaction intermediates was performed on-line by the ESI-MS equipment during the oxidation of the methylene blue dye for 60 min of reaction (Fig. 3). It was possible that after 60 min of reaction strong signals corresponding to $m/z = 300$, 316, 347, and 384 are detected, due to successive hydroxylation of the dye structure. The previous treatment of the niobia with H_2O_2 leads to much higher catalytic activity for the synthetic niobia. Actually, from Fig. 3, the increasing number of reaction intermediates can clearly be observed after the same time of reaction and also the complete disappearing of the signal $m/z = 284$.

Reaction mechanism: substrate point of view

The intermediate structures are reported in Fig. 4. The calculation of the Gibbs free energy for the stability of the intermediates was performed by the method implemented in the *Gaussian98* package [17]. The resulting energies values are shown in Table 1. Previous works [18, 19] put in evidence that intense fragment corresponding to $m/z = 300$ (Fig. 3) results from the hydroxylation in the aromatic ring. According to data listed in Table 1, it can be observed that the hydroxyl group at C2 position is about +3.30, +6.65, +7.86, and +8.68 kcal mol^{-1} more stable than the alternative C3, C5, N, and S, respectively.

In order to get a deeper insight about the sing m/z 300, we calculated at DFT level the Gibbs free energy for the stability of some possible isomers with m/z 300. From our data, we may note that in the most stable fragment the hydroxyl group is at C2 position. This certainly corroborates our previous findings [18, 19] and reinforces the

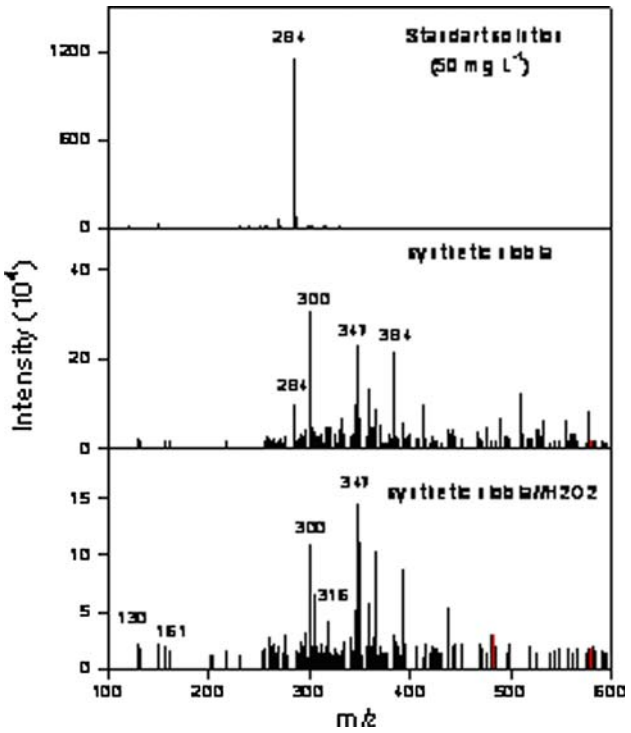

Fig. 3 ESI mass spectra in the positive ion mode for monitoring the oxidation of methylene blue dye in water by the synthetic niobia at different reactions times

earlier reaction mechanism proposed, which involves the generation of hydroquinone or hydroquinone-like intermediate and the redox cycle of hydroquinone/quinone in the Fenton reaction. That is an unstable key-intermediate that points out the quick and high probability of rupture of both chemical bonds C1–C2 and C5–C6 (Fig. 4).

Further calculations revealed that the hydroxylation occurs at C3, which explains the resulting intense fragment corresponding to $m/z = 316$. Thus, the compounds **II** and **III** (Fig. 4) are supposed to be stables and the reaction path may still involve other hydroxylations. From these results, the third hydroxylation would more likely occur at 5′ position. This is a critical step, as it would simultaneously

Table 1 Gibbs free energy of **II** and **III** intermediates using B3LYP/6-31+G(d,p)

Intermediate	Hydroxyl position	ΔG (kcal mol^{-1})
II	2	0.00
	3	+3.30
	N	+7.86
	S	+8.68
	5	+ 6.04
III	2, 2′	0.00
	2, 5′	+34.69
	3, 2′	+11.73
	3, 3′	+14.26
	3, 5′	+3.25
	5, 5′	+21.22

lead to the formation of hydroquinone or hydroquinone-like intermediates generated by the $^{\bullet}$OH attack. This is an unstable key-intermediate that points out the quick and high probability of rupture of both chemical bonds C1–C2 and C5–C6 (Fig. 4). This could justify the formation of **V** ($m/z = 130$). Nevertheless the presence of $^{\bullet}$OH in the reaction medium the oxidation of **V** probably occurs, which consequently generates the **VI** stable specie, with $m/z = 160$. These calculations show a good agreement with the experimental data (Fig. 3). Surprisingly, the fragmentation pathway is quite similar to the one described in our previous study [19]. This could strongly suggest that the reaction with niobia catalyst initializes by the activation of H_2O_2 to produce an $^{\bullet}$OH radical.

Reaction mechanism: catalyst point of view

In an ab initio calculation of the type reported here, there is a primary consideration: the choice of the basis set and the form of the exchange-correlation functionals. For carbon and oxygen, we have used a large all electron 6-311++G** [20] basis set, and, for niobium, we have

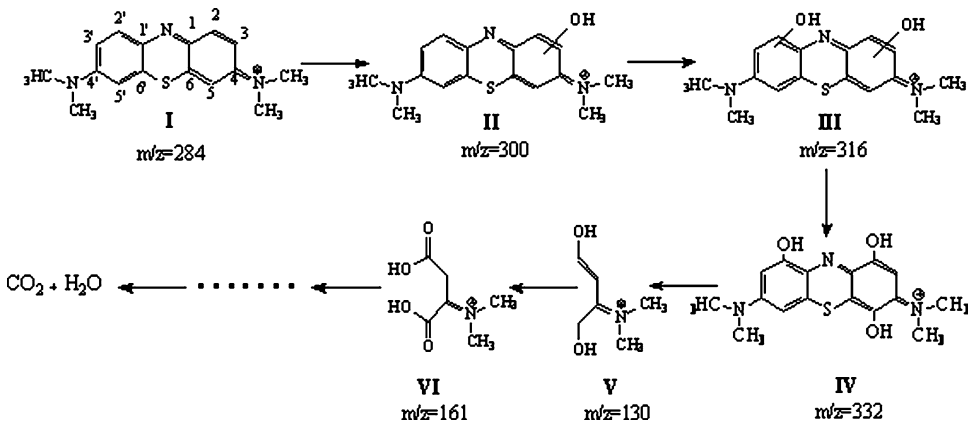

Fig. 4 Chemical structure of the reaction intermediates

used a pseudopotential and an associated basis set [21]. From our calculation, a good agreement between the calculated and experimental geometry for niobium complex [22] was observed. After the optimization of the selected conformers, a force constant calculation was carried out to assure that the conformers reported in Figs. 1 and 4 are all local minima and that the structures reported in Tables 1 and 2 are intermediates [23]. In order to carry out the calculations to obtained the energy of the intermediates, **C-I** and **C-II**, the low energy associated to the intermediates was attributed, for instance, to the forming of strong n_{Nb}/σ^*_{O-O}, n_{Nb}/σ^*_{O-H}, $\sigma_{O-H}/\sigma^*_{O-O}$, $\sigma_{O-O}/\sigma^*_{O-H}$, and $\sigma_{Nb-O}/\sigma^*_{O-H}$ interactions (Table 3).

Non-bonded interactions play an important role in the complex stabilization [24]. For instance, studies with 69 additional published crystal structures of organic, inorganic, and organometallic compounds containing divalent sulfur (S bonded to two ligands, Y and Z, different from H) revealed that, in the lattice, electrophiles tend to approach the sulfur atom roughly 20° from a line perpendicular to the Y–S–Z atoms plane, whereas nucleophiles tend to approach approximately along the extension of one of the sulfur covalent bonds [25, 26]. We believe that these regularities portray features of the electron distribution and indicate the preferred direction of approximation of electrophiles and nucleophiles, as well as the preferred direction for non-bonded interactions. These features are not observed with the same intensity in the case of niobium [27]. According to the data shown in Table 2 and Fig. 5, it can be noted that, in comparison with **C-I**, **C-II** has a higher energy barrier for its formation. In addition, statistically, it much more probable to form a complex involved with two molecules than tree. In fact, it is observed experimentally that there is a smaller activation barrier associated to **C-I** [19]. The generated peroxo complex **C-I** has two reaction pathways possible. The first one, it is the formation of the **C-I$_1$** (intermediate complex 1) and the second one is the formation **C-I$_2$**. Several papers describe powder XRD of Nb and Ta peroxo complexes [28–31]. Thus the peroxo complex of niobium probably occurs in solution. Our previous experimental findings are in line with this conclusion too [18, 19]. We select the cluster NbO_6 in order to model the outmost surface layer of the catalysts due to X-ray results of this kind structure [27]. Therefore, the reaction mechanism, as well as the relative energies, can be well established with the model studied of peroxo complex. This theoretical consideration is a good agreement with experimental results from other groups [22, 32].

In order to investigate the oxidation state of niobium atom in the peroxo complex, we performed theoretical calculation on the reaction pathway of the hydroperoxo complex (**C-I**) in three possible oxidation states of niobium [33]. Thus to get more insight, the electrostatic charges were determined so as to reproduce the B3LYP/6-311++G** quantum molecular mechanical electrostatic potential [34]. This means that it was necessary to produce charges that fit into the electrostatic potential at points selected according to the CHelpG scheme [35, 36]. As expected, the most favorable niobium states of oxidation either +5 or 3+ in the initial complex what is consistent with the literature [33]. We are quite aware of the limitations of this cluster model, but as shown in other publications, at least for small sized substrates, the larger clusters do not introduce any changes in the mechanism [37]. Therefore, the mechanism of the reaction, as well as the relative energies, can be well established with the Nb complex model. Furthermore, it is well known that Nb atom in niobia is limited almost entirely to the state of oxidation of +5. However, it is an interesting fact that niobium develops for 4+ charge in both peroxo complexes, in other words **C-I(+4)** and **C-II(+4)** are the most stable complexes. This behavior remains in the other transformation steps of reaction. Nevertheless when the rupture of the O–O or O–H chemical bonds (Fig. 5) occurs, the most favorable complex formed is **C-I$_1$(+5)**. Those theoretical and experimental results suggest the formation of reactive species, partially reduced niobia, on niobia surface with peroxide. The data showed that the Nb_2O_5 is a potential catalyst for the hydrogen peroxide decomposition producing hydroxyl radical ($^{\bullet}$OH) by the Fenton-like system. In line with that observation, we can propose the scheme described in Fig. 6 for the behavior of niobia species on oxidation reactions. Comparison between theoretical and experimental data shows that many similarities exist. In both situations, indeed, the most likely reaction mechanism involves, as a first step the formation of a stable complex whose formation is dominated by the donor–acceptor mechanism. The charge upon niobium (Table 2) after interaction is reduced suggesting a contribution of peroxide → metal charge transfer, which agrees to the known surface acidity behavior. Otherwise, Lewis acids

Table 2 Relative Gibbs free energy among the intermediates with the system charge +3, +4, and +5 using B3LYP/6-31+G(d,p)

Charge system	Complex	C-I	C-II	C-I$_1$	C-I$_2$
+3	+1.81	+28.14	+29.44	+1.23	+1.50
+4	+20.65	0.00	0.00	0.00	+1.45
+5	0.00	+24.06	+2.18	+1.96	0.00

Table 3 Orbital interaction energies ($\Delta E2$) for **C-I** compounds

Charge system	n_{Nb}/σ^*_{O-O}	n_{Nb}/σ^*_{O-H}	$\sigma_{O-H}/\sigma^*_{O-O}$	$\sigma_{O-O}/\sigma^*_{O-H}$	$\sigma_{Nb-O}/\sigma^*_{O-H}$
+3	0.24	1.73	6.73	4.58	0.80
+4	0.10	1.93	6.71	4.58	8.24
+5	0.31	1.71	6.72	6.80	0.76

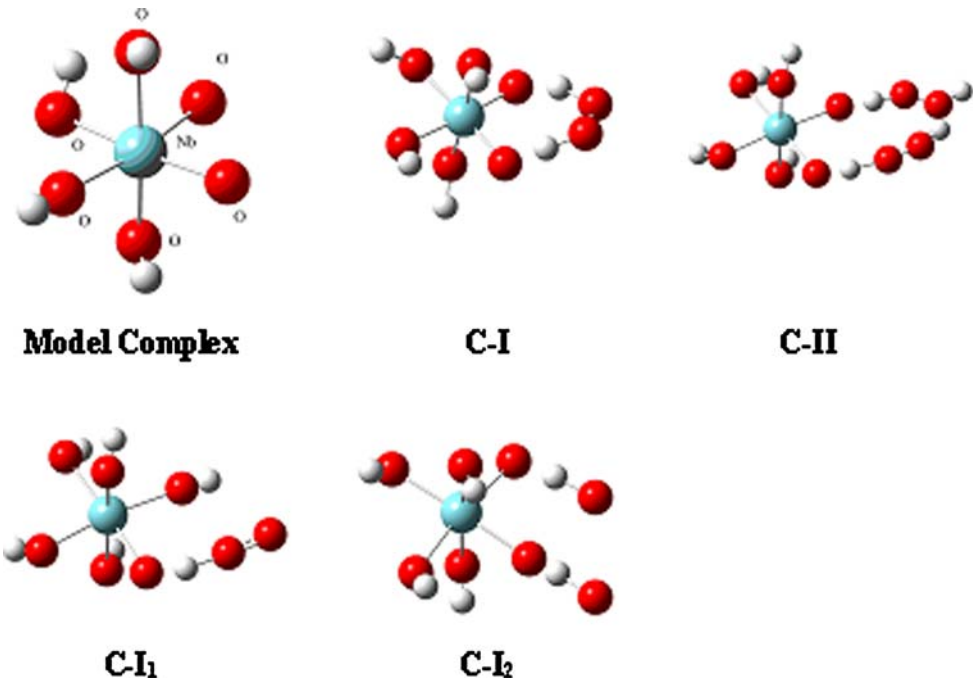

Fig. 5 Model structures for the catalyst

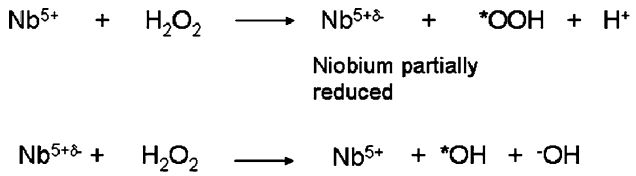

Fig. 6 Proposed catalytic cycle

will cause some changes in the orbital occupancies. Therefore the occupancy of donors orbitals is of major interest. The Natural Bond Orbital (NBO) analysis occupancies of the **C-I** complex show that the most significant change upon interaction is the decrease in occupancy of O–H chemical bond from 1.94 to 1.62.

It is well known from literature that Nb^{4+} is much more unstable than Nb^{5+} [33, 38]. Nevertheless, the partial reduction of the niobium can be take place by the previous treatment with hydrogen peroxide and the formation of peroxo complex on niobia surface by the donor–acceptor mechanism. In this case, H_2O_2 may act as reducing agent to produce a more active niobium phase, which can form the hydroxyl radical ($^{\bullet}OH$), according to the equations reported in Fig. 6.

The results from Fig. 2 are agreement with this explanation because it shows a small activity for the pure niobia (no previous treatment with H_2O_2) up to 90 min of reaction. Probably before this time the partial reduction of niobia does not occur. But, after 90 min the activity catalytic is similar that compared with material previously treated, suggesting the peroxo complex formation in situ.

Thus, to determine the relative chemical stability of both **C-I**, **C-I$_1$**, and **C-I$_2$** involved, NBO analyses were carried out using the second-order perturbation theory (Eq. 1), which estimates the stabilization as the ratio between the square of the Fock matrix element and the energy difference between the interacting orbitals [13, 39].

The energy difference between donor (σ_{Nb-O}) and acceptor (σ^*_{O-H}) orbitals in the denominator decrease from **C-I(+4)** to **C-I(+5)** (8.24 and 2.65 kcal mol^{-1}, respectively). Thus, the smaller $\Delta E2$ values is obtained for **C-I(+3)** (Table 3). The energy difference due to the Fock matrix element is small. Therefore, the magnitude of the interaction is dominated by the energy difference between the acceptor and the donor orbitals (which appears in Eq. 1 as its second power).

$$\Delta E2 = \frac{qF_{ij}^2}{(\varepsilon_i - \varepsilon_j)}. \quad (1)$$

From Table 3, we could note that **C-I** complex is stabilized by n_{Nb}/σ^*_{O-O}, n_{Nb}/σ^*_{O-H}, $\sigma_{O-H}/\sigma^*_{O-O}$, $\sigma_{O-O}/\sigma^*_{O-H}$, and $\sigma_{Nb-O}/\sigma^*_{O-H}$ interactions, which were not present in the *model complex* (Fig. 5). Thus, the formation of the peroxo complex **C-I(+4)** could be attributed the strong $\sigma_{Nb-O}/\sigma^*_{O-H}$ interaction (8.24 kcal mol^{-1}) (hyperconjugation between Nb–O chemical bond and hydroxyl chemical bond).

Furthermore, it was observed that **C-I$_1$(+4)** is more stable than **C-I$_2$(+5)**, **C-I$_2$(+4)**, and **C-I$_2$(+3)** about 2.64, 4.09, and 4.34 kcal mol^{-1}, respectively. These results demonstrate that the electron attack will be preferential on the O–H chemical bond, forming a peroxide molecule (Fig. 6). The $\sigma_{Nb-O}/\sigma^*_{O-H}$ interaction is about 5.30 kcal mol^{-1} more effective in stabilizing the **C-I$_2$(+4)** than **C-I$_2$(+5)**. One of

the contributions is due to the greater overlap between the O–H orbital and the Nb–O chemical bond of the catalyst.

Conclusion

There have been many studies aimed at developing a physical understanding of the new catalyst on the oxidation reaction. Here we highlight some basic trends encountered in the literature, the results in this paper show that niobium is a good catalyst for the oxidation of organic dyes, and that the previous treatment of the material with hydrogen peroxide improves the catalytic activity. The better catalytic activity of the material after the previous treatment with H_2O_2 may be due to the hydroxyl radical highly reactive generated with the partial reduction of niobium.

Acknowledgement We are grateful to the FAPEMIG and CNPq Brazilian agencies for funding part of this work and CENAPAD-SP for the computational facilities.

References

1. Tanabe K (2003) Catal Today 78:65. doi:10.1016/S0920-5861(02)00343-7
2. Tanabe K, Okazak SI (1995) Appl Catal 133:191. doi:10.1016/0926-860X(95)00205-7
3. Pereira EB, Pereira MM, Lam YL, Perez CAC, Schmal M (2000) Appl Catal A Gen 197:99
4. Petre AL, Perdigón-Melón JA, Gervasini A, Auroux A (2003) Catal Today 78:377
5. Nowak I, Ziolek M (1999) Chem Rev 99:3603
6. Lu M, Chen J, Huang H (2002) Chemosphere 46:131
7. Cornell RM, Schwertmann U (2003) The iron oxides, 3rd edn. Weinheim-VHC, New York
8. Frisch MJ, Trucks GW, Schlegel HB, Scuseria GE, Robb MA, Cheeseman JR, Zakrzewski VG, Montgomery JA Jr, Stratmann RE, Burant JC, Dapprich S, Millam JM, Daniels AD, Kudin KN, Strain MC, Farkas O, Tomasi J, Barone V, Cossi M, Cammi R, Mennucci B, Pomelli C, Adamo C, Clifford S, Ochterski J, Petersson GA, Ayala PY, Cui Q, Morokuma K, Malick DK, Rabuck AD, Raghavachari K, Foresman JB, Cioslowski J, Ortiz JV, Baboul AG, Stefanov BB, Liu G, Liashenko A, Piskorz P, Komaromi I, Gomperts R, Martin RL, Fox DJ, Keith T, Al-Laham MA, Peng CY, Nanayakkara A, Challacombe M, Gill PMW, Johnson B, Chen W, Wong MW, Andres JL, Gonzalez C, Head-Gordon M, Replogle ES, Pople JA (1998) Gaussian 98, revision A.9. Gaussian, Inc., Pittsburgh, PA
9. Da Cunha EFF, De Alencastro RB, Ramalho TC (2004) J Theor Comp Chem 31:1
10. da Silva RR, Ramalho TC, Santos JM, Figueroa-Villar JD (2006) J Phys Chem A 110:1031
11. Barone V, Cossi M, Tomasi J (1998) J Comp Chem 19:404
12. Tomasi J, Mennucci B, Cammi R (2005) Chem Rev 105:2999
13. Wang P, Zhang YL, Streitwieser A (1991) J Am Chem Soc 113:55
14. Reed E, Curtiss LA, Weinhold F (1988) Chem Rev 88:899
15. Neubauer-Guenther P, Giesen TF, Schlemmer S (2007) J Chem Phys 127:014313
16. Gonzalez C, Schlegel HB (1989) J Chem Phys 90:2154
17. Frisch MJ, Trucks GW, Schlegel HB, Scuseria GE, Robb MA, Cheeseman JR, Montgomery JA Jr, Vreven T, Kudin KN, Burant JC, Millam JM, Iyengar SS, Tomasi J, Barone V, Mennucci B, Cossi M, Scalmani G, Rega N, Petersson GA, Nakatsuji H, Hada M, Ehara M, Toyota K, Fukuda R, Hasegawa J, Ishida M, Nakajima T, Honda Y, Kitao O, Nakai H, Klene M, Li X, Knox JE, Hratchian HP, Cross JB, Bakken V, Adamo C, Jaramillo J, Gomperts R, Stratmann RE, Yazyev O, Austin AJ, Cammi R, Pomelli C, Ochterski JW, Ayala PY, Morokuma K, Voth GA, Salvador P, Dannenberg JJ, Zakrzewski VG, Dapprich S, Daniels AD, Strain MC, Farkas O, Malick DK, Rabuck AD, Raghavachari K, Foresman JB, Ortiz JV, Cui Q, Baboul AG, Clifford S, Cioslowski J, Stefanov BB, Liu G, Liashenko A, Piskorz P, Komaromi I, Martin RL, Fox DJ, Keith T, Al-Laham MA, Peng CY, Nanayakkara A, Challacombe M, Gill PMW, Johnson B, Chen W, Wong MW, Gonzalez C, Pople JA (2004) Gaussian03, revision C.02. Gaussian, Inc., Wallingford, CT
18. Oliveira LCA, Ramalho TC, Gonçalves M, Cereda F, Carvalho KT, Nazzarro MS, Sapag K (2007) Chem Phys Lett 446:133
19. Oliveira LCA, Ramalho TC, Gonçalves M, Sapag K (2007) Appl Cat A Gen 316:117
20. El-Taher S, Hilal RH (2007) Int J Quantum Chem 2001(20):242
21. Fuentealba P, Preuss H, Stoll H, Szentpaly LV (1989) Chem Phys Lett 89:418
22. Bayot D, Tinant B, Devillers M (2003) Catal Today 78:439
23. Ramalho TC, Taft CA (2005) J Chem Phys 123:054319
24. Ramalho TC, Martins TLC, Borges LEP, Figueroa-Villar JD (2003) Int J Quantum Chem 95:267
25. Wang X, Houk KN, Spichty M, Wirth T (1999) J Am Chem Soc 121:8567
26. Rosenfield RE, Pathasatathy R (1977) J Am Chem Soc 99:4860
27. Wirth T, Fragale G, Spichty M (1998) J Am Chem Soc 120:3376
28. Haxhillazi G, Haeuseler H (2004) J Solid State Chem 177:3045
29. Selezneva KI, Nisel'son LA (1968) Russ J Inorg Chem 13:45
30. Boehm G (1926) Z Krist 63:319
31. Shchelokov RN, Traggeim EN, Varfolomeev MB, Michnik MA, Morozova SV (1972) Russ J Inorg Chem 17:1273
32. Burcham LJ, Datka J, Wachs IE (1999) J Phys Chem B 103:6015
33. Bayot D, Devillers M (2006) Coord Chem Rev 250:2610
34. Ramalho TC, de Alencastro RB, La-Scaleac MA, Figueroa-Villar JD (2004) Biophys Chem 110:267
35. Singh UC, Kollman PA (1984) J Comput Chem 5:129
36. Goldman P, Koch RL, Yeung TC (1986) Biochem Pharmacol 35:43
37. Milas I, Nascimento MAC (2003) Chem Phys Lett 373:379
38. Mangham RI, Petuskey WT (2008) J Mater Sci 43:621. doi:10.1007/s10853-007-2710-0
39. Salzneer U, Schleyer PV (1993) J Am Chem Soc 115:10231